

LONGITUDINAL AND TRANSVERSE WAKE-FIELDS OF A  
RELATIVISTIC PARTICLE IN A DIELECTRIC-LINED STRUCTURE

G. Dôme

CERN - 1211 Geneva 23, Switzerland

Abstract

A complete study is made of the longitudinal and transverse wake fields produced by an ultra-relativistic particle in a dielectric-lined structure. If, for use as a wake field accelerator, this structure has a relative dielectric constant (between 2 and 3) optimized for producing longitudinal effects, it will at the same time produce transverse effects; moreover, the peak values of both longitudinal and transverse wake potentials per unit length excited by a point charge are comparable to those in a disk-loaded structure with the same transverse dimensions.

Note: Due to the lack of space Fig. 2 has been dropped.

Infinite dielectric-lined structure

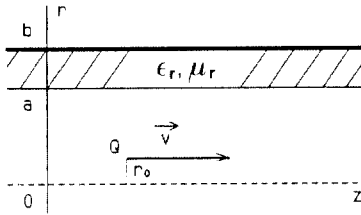


Fig. 1 Infinitely conducting pipe of inner radius  $b$  loaded with a dielectric having a beam-hole radius  $a$ . A point charge  $Q$  moves with longitudinal velocity  $v$  in the hole.

The longitudinal electric field  $E_z$  is a superposition of components with  $m$ -fold rotational symmetry around the pipe axis.

If  $\left| \frac{ka}{\beta\gamma} \right| \ll 1$ , the  $m$ -component of the second part of  $E_z$  reads in frequency domain [2]:

$$E_z(\omega) = -\frac{Q}{\pi_0 c} e^{-j\frac{\omega}{v}z} \frac{(m+1)F}{jka^2} \left\{ 1 - \frac{A}{(ka)^2} + \frac{B}{ka} \left[ \frac{\epsilon_r}{\epsilon_r + \mu_r} D_m(k_r b) + \frac{\mu_r}{\epsilon_r + \mu_r} D'_m(k_r b) \right] \right\}^{-1} \frac{N_{||}(\omega)}{\epsilon_m} \quad \left| \frac{ka}{\beta\gamma} \right| < 1 \quad (3)$$

$$\text{where } F \approx 1, \quad A = m(m+1) \left( \epsilon_r \mu_r + \frac{1}{\beta^2} \right), \quad B = (m+1)(\epsilon_r + \kappa_r) \quad \text{with } \begin{cases} \kappa_r = \mu_r & \text{when } m > 0 \\ \kappa_r = \epsilon_r & \text{when } m = 0 \end{cases} \quad (4)$$

When  $m = 0$ , the weights  $\frac{\epsilon_r}{\epsilon_r + \mu_r}, \frac{\mu_r}{\epsilon_r + \mu_r}$  must be taken as 1,0.

With  $\epsilon_r = \mu_r = 1$  and  $\beta = 1$ , the minimum values of (4) are  $A = 2m(m+1)$  and  $B = 2(m+1)$ .

In (3),

$$D_m(k_r b) = \frac{\begin{vmatrix} J'_m(k_r a) & Y'_m(k_r a) \\ J_m(k_r b) & Y_m(k_r b) \end{vmatrix}}{\begin{vmatrix} J_m(k_r a) & Y_m(k_r a) \\ J_m(k_r b) & Y_m(k_r b) \end{vmatrix}} = \frac{\begin{vmatrix} H_m^{(1)}(k_r a) & H_m^{(2)}(k_r a) \\ H_m^{(1)}(k_r b) & H_m^{(2)}(k_r b) \end{vmatrix}}{\begin{vmatrix} H_m^{(1)}(k_r a) & H_m^{(2)}(k_r a) \\ H_m^{(1)}(k_r b) & H_m^{(2)}(k_r b) \end{vmatrix}} \quad D'_m(k_r b) = \frac{\begin{vmatrix} J'_m(k_r a) & Y'_m(k_r a) \\ J'_m(k_r b) & Y'_m(k_r b) \end{vmatrix}}{\begin{vmatrix} J_m(k_r a) & Y_m(k_r a) \\ J'_m(k_r b) & Y'_m(k_r b) \end{vmatrix}} = \frac{\begin{vmatrix} H_m^{(1)}(k_r a) & H_m^{(2)}(k_r a) \\ H_m^{(1)}(k_r b) & H_m^{(2)}(k_r b) \end{vmatrix}}{\begin{vmatrix} H_m^{(1)}(k_r a) & H_m^{(2)}(k_r a) \\ H_m^{(1)}(k_r b) & H_m^{(2)}(k_r b) \end{vmatrix}} \quad (5)$$

where  $J_m(x), Y_m(x)$  are Bessel functions and  $H_m^{(1)}(x), H_m^{(2)}(x)$  are Hankel functions of order  $m$ ;  $m=0$  corresponds to an accelerating mode,  $m>0$  corresponds to deflecting modes. Equation (3) has also been obtained recently by Ng [3].

Finally, with the condition  $\left| \frac{ka}{\beta\gamma} \right| \ll 1$ , (2) reduces to

$$N_{||} = \left( \frac{r}{a} \right)^m \left( \frac{r_0}{a} \right)^m \epsilon_m \cos m(\varphi - \varphi_0) \quad \left| \frac{ka}{\beta\gamma} \right| < 1 \quad (6)$$

which is independent of frequency.

In the region  $0 < r < a$ , the synchronous wave (i.e. the wave whose phase velocity is equal to the particle velocity  $v$ ) is made up of two parts:

The first part, which is a solution of the inhomogenous Helmholtz equation, is identical to the synchronous wave in a conducting cylinder of radius  $a$ . It only involves the wave number  $k = \omega / c$  through a radial propagation constant  $jk / (\beta\gamma)$ .

The second part, which is a solution of the homogeneous Helmholtz equation, involves  $k$  also through a radial propagation constant  $k_r$  which is characteristic of the dielectric:

$$k_r = k \left( \epsilon_r \mu_r - \frac{1}{\beta^2} \right)^{1/2} = \frac{k}{\beta} \left( \epsilon_r \mu_r \beta^2 - 1 \right)^{1/2} \quad (1)$$

The exciting charge  $Q$  has transverse coordinates  $(r_0, \varphi_0)$ . In order to shorten the notation we let

$$N_{||}(\omega) = \frac{I_m \left( \frac{kr}{\beta\gamma} \right) I_m \left( \frac{kr_0}{\beta\gamma} \right)}{I_m \left( \frac{ka}{\beta\gamma} \right) I_m \left( \frac{ka}{\beta\gamma} \right)} \epsilon_m \cos m(\varphi - \varphi_0) \quad (2)$$

where  $\epsilon_m$  is Neumann's symbol ( $\epsilon_m = 1$  when  $m = 0$ ,  $\epsilon_m = 2$  when  $m \neq 0$ ) and  $I_m(x), K_m(x)$  are modified Bessel functions of order  $m$ .

It should be noticed that in contrast to our previous paper [1],  $\epsilon_m$  is now included in the definition of  $N_{||}(\omega)$ .

In the following, we assume that  $\beta^2 > \frac{1}{\epsilon_r \mu_r}$ , which means that the velocity of the exciting charge is above the threshold for Cherenkov radiation in the dielectric; by (1) this case corresponds to  $k_r$  being real. More precisely, since causality requires that  $\omega$  be thought of as a complex quantity  $(\omega - j\epsilon)$  with  $\epsilon > 0$ ,  $k_r$  should also be considered as a complex quantity having a small negative imaginary part. Therefore, from (5):

$$\lim_{b \rightarrow \infty} D_m(k, b) = \lim_{b \rightarrow \infty} D'_m(k, b) = \frac{H_m^{(2)}(k, a)}{H_m^{(2)}(k, a)} \quad (7)$$

#### Longitudinal wake potential per unit length of the structure

For a particle which follows the charge Q with the same velocity  $v$ , at a distance  $s$  behind Q, and at transverse coordinates  $(r, \varphi)$ , this wake potential reads

$$w_{||}(s) = -\frac{1}{Q} \int_{-\infty}^{+\infty} \frac{d\omega}{2\pi} e^{j\frac{\omega s}{v}} \cdot e^{j\frac{\omega r}{v}} E_r(\omega) \quad (8)$$

With (3) it can be written as

$$w_{||}(s) = \frac{N_{jc}(m+1)F}{\epsilon_m \pi \epsilon_0 a^2} \cdot v(s) \quad \left[ \frac{V}{C} m^{-1} \right] \quad \left| \frac{ka}{\beta\gamma} \right| < 1 \quad (9)$$

where

$$v(s) = \frac{1}{2\pi j} \int_{-\infty}^{+\infty} \frac{dz}{z} e^{j\frac{z s}{\beta^2}}$$

$$\cdot \left\{ 1 - \frac{A}{(k, a)^2} + \frac{B}{k, a} \left[ \frac{\epsilon_r}{\epsilon_r + \mu_r} D_m(k, b) + \frac{\mu_r}{\epsilon_r + \mu_r} D'_m(k, b) \right] \right\}^{-1} \quad (10)$$

When  $b = \infty$ ,  $D_m(k, b)$  and  $D'_m(k, b)$  may both be replaced by (7), so that (10) reduces to

$$v(x) = \frac{1}{2\pi j} \int_{-\infty}^{+\infty} \frac{dz}{z} e^{jzx} \left[ 1 - \frac{A}{z^2} + \frac{B}{z} \frac{H_m^{(2)}(z)}{H_m^{(2)}(z)} \right]^{-1} \quad (11)$$

$$\text{where } z = k, a, \quad x = \frac{s}{a} (\epsilon_r \mu_r \beta^2 - 1)^{-\frac{1}{2}} \quad (12)$$

Using properties of Bessel functions, one can reduce (11) to

$$v(x) = H(x) \frac{1}{\pi} \text{Im} \int_0^{\infty} dz e^{jzx} \left[ z - \frac{A}{z} + B \frac{H_m^{(2)}(z)}{H_m^{(2)}(z)} \right]^{-1} \quad (13)$$

where  $H(x)$  is Heaviside's unit step function.

To obtain a formula suitable for numerical computation, it suffices to express (13) in terms of  $J_m(z)$ ,  $Y_m(z)$ .

The behaviour of  $v(x)$  for  $x \rightarrow 0+$  can be obtained by using the asymptotic expansion of the Hankel functions in (11); remembering that the integral should be taken slightly below the real axis, this yields

$$v(x) = H(x) \left[ 1 - Bx + \left( B^2 - \frac{B}{2} - A \right) \frac{x^2}{2} + \dots \right] \quad (14)$$

where, from (4) and (12):

$$Bx = (m+1)(\epsilon_r + \mu_r)(\epsilon_r \mu_r \beta^2 - 1)^{-\frac{1}{2}} \frac{s}{a} \quad (15)$$

The least fall off of  $w_{||}(s)$  with  $s/a$  occurs when

$(\epsilon_r + \mu_r)(\epsilon_r \mu_r \beta^2 - 1)^{-\frac{1}{2}}$  is minimum. As a function of  $\epsilon_r$ , this happens when

$$\epsilon_r = \frac{2}{\mu_r \beta^2} \quad (m=0) \quad \text{or} \quad \epsilon_r = \frac{2}{\mu_r \beta^2} + \mu_r \quad (m>0) \quad (16)$$

For  $\beta=1$  and  $\mu_r=1$ , this corresponds to  $\epsilon_r=2$  when  $m=0$  and  $\epsilon_r=3$  when  $m>0$ ; in both cases it corresponds to  $A=mB$  and  $B=4(m+1)$ .

The precise shape of  $v(x)$  is obtained by numerical integration of (13); the results are shown in Fig. 2. It is seen that  $v(x)$  changes sign  $(m+1)$  times before going monotonically to zero.

When  $B$  increases, the first zero of  $v(x)$  is steadily shifted to the origin, whereas the  $m$  subsequent zeros barely change position.

When  $b < \infty$ , the integrand in (10) has a simple infinity of poles at  $k = \pm k_n$ , with positive residues  $R_n$  (the same at  $k_n$  and  $-k_n$ ). Taking the integral with respect to  $k$  slightly below the real axis transforms (10) into

$$v(s) = H(s) \sum_{n=0}^{\infty} 2R_n \cos\left(k_n \frac{s}{\beta}\right) \quad R_n > 0, \quad \frac{b}{a} < \infty \quad (17)$$

The electromagnetic wave front created by the exciting charge Q needs some time to be reflected by the wall at  $r=b$  and reach the test particle at a distance  $s$  behind Q. Using (10) it can be shown that as long as

$$s(\epsilon_r \mu_r \beta^2 - 1)^{-\frac{1}{2}} \leq 2(b-a) \quad \text{i.e.} \quad x \leq 2\left(\frac{b}{a} - 1\right) \quad (18)$$

the test particle does not feel the presence of the outer wall at  $r=b$ ; therefore  $v(s)$  does not depend on  $b$  in that range of  $s$ . In other words, within the range (18) of  $s$ , the general expression (17) is identical to the expression (11) valid for any  $s$  when  $b = \infty$ ; in particular, from (14) we always have  $v(0+) = 1$  and therefore

$$\sum_{n=0}^{\infty} 2R_n = 1 \quad (19)$$

where [2]  $R_n$  decreases as  $k_n^{-2}$  for large  $n$ . All these properties have been verified by numerical computation of (17) for  $b/a = 2$  and 3. However, when  $b$  is finite  $v(s)$  does not tend to zero when  $s \rightarrow \infty$ ; indeed, from (17)  $v(s)$  is an almost periodic function of  $s$ , and as such it comes back an infinity of times to the neighbourhood of any value which it has taken since  $s=0$ . The physical reason is that subsequent reflections from the outer wall keep arriving at every multiple of the bound (18).

When  $b/a \gg 1$  (say  $b/a > 2$ ),  $R_n$  decreases slowly with  $n$ ; by (19) even the first  $R_n$ 's are then rather small.

When  $b \rightarrow a$ , all frequencies  $k_n$  in (17) go to  $\infty$ ; it can be shown [2] that all residues  $R_n$  tend to zero except the first one ( $n=0$ ) which tends to 1/2. In that case  $v(x)$  reduces to a single cosine with unit amplitude.

#### Transverse wake potential per unit length of the structure

The transverse wake potential  $\tilde{w}_{\perp}(s)$  can be deduced at once from the longitudinal wake potential  $w_{||}(s)$  by using the Panofsky-Wenzel theorem:

$$\beta \frac{\partial}{\partial s} \tilde{w}_{\perp}(s) = \text{grad}_{\perp} w_{||}(s) \quad (20)$$

Letting:

$$\tilde{N}_{\perp}(\omega) \equiv a \cdot \text{grad}_{\perp} N_{||}(\omega) \quad (21)$$

we obtain from (9):

$$\bar{w}_{\perp}(s) = \frac{\tilde{N}_{\perp 0}}{\epsilon_m} \frac{F}{\pi \epsilon_0 a^2} \cdot \frac{1}{\beta} \frac{(\epsilon_r \mu_r \beta^2 - 1)^{\frac{1}{2}}}{(\epsilon_r + \kappa_r)} u(x) \left[ \frac{V}{C} \text{m}^{-1} \right] \left| \frac{ka}{\beta \gamma} \right| < 1 \quad (22)$$

where

$$u(x) = \int_{-\infty}^x v(x) B dx = H(x) \int_0^x v(x) B dx \quad (23)$$

From (6) and (21) we have

$$N_{\perp 0} \Big|_{\varphi} = m \left( \frac{r}{a} \right)^{m-1} \left( \frac{r_0}{a} \right)^m \epsilon_m \frac{\cos m(\varphi - \varphi_0)}{-\sin m(\varphi - \varphi_0)} \left| \frac{ka}{\beta \gamma} \right| < 1 \quad (24)$$

Within the range (18) of  $s$ , the integral (23) is obtained directly from (11) as

$$u(x) = \frac{B}{2\pi} \int_{-\infty}^{+\infty} \frac{dz}{(jz)^2} e^{jzx} \left[ 1 - \frac{A}{z^2} + \frac{B}{z} \frac{H_m^{(2)}(z)}{H_m^{(2)}(z)} \right]^{-1} \quad (25)$$

The first maximum of  $u(x)$  is slightly less than 1. When  $B \rightarrow \infty$  it tends to 1, at a position of  $x$  which is shifted to the origin, whereas the  $m$  zeros of  $u(x)$  (not counting the origin) are only slightly affected by a change in  $B$ . From (22), the peak of the transverse wake potential is thus approximately proportional to

$$\frac{1}{\beta} \frac{(\epsilon_r \mu_r \beta^2 - 1)^{\frac{1}{2}}}{(\epsilon_r + \kappa_r)} \leq \begin{cases} \frac{\mu_r \beta}{4} & \text{when } m = 0 \\ \frac{\mu_r \beta}{2} (1 + \mu_r^2 \beta^2)^{-\frac{1}{2}} & \text{when } m > 0 \end{cases} \quad (26)$$

The maximum is reached for the value of  $\epsilon_r$  given by (16), i.e. the same value which optimizes the longitudinal wake potential.

Taking  $F = \mu_r = \beta = 1$ , from (22), (26) and Fig. 2 we deduce that

$$w_{\perp}(s) \leq \frac{N_{\perp 0}}{\epsilon_m} \frac{1}{4\pi \epsilon_0 a^2} \sqrt{\epsilon_m} u_{\max}(x) \approx \frac{N_{\perp 0}}{\epsilon_m} \frac{1}{4\pi \epsilon_0 a^2} \quad (27)$$

This relation applies if the maximum of  $u(x)$  is reached before the limit (18) for  $x$ , i.e. if the position  $x_{\max}$  of the maximum is such that

$$2 \left( \frac{b}{a} - 1 \right) > x_{\max} \quad (28)$$

where  $x_{\max}$  is the first zero of  $v(x)$ ; let us remember that  $x_{\max}$  depends on  $B$  and tends to zero when  $B \rightarrow \infty$ . A value of  $b/a$  smaller than the limit (28) would decrease the upper bound (27).

As it appears in Fig.2,  $u(x)$  changes sign  $m$  times before going monotonically to zero.

**When  $s$  is larger than the bound (18)**, the reflection at the outer wall  $r=b$  begins to influence the test particle, and we have to integrate (17) with respect to  $x$ . Remembering (12) and (23) this yields

$$u(x) = H(x) B \beta (\epsilon_r \mu_r \beta^2 - 1)^{-\frac{1}{2}} \sum_{n=0}^{\infty} \frac{2R_n}{k_n a} \sin \left( k_n \frac{s}{\beta} \right) \quad (29)$$

which is an almost periodic function of  $s$ .

When  $b \rightarrow a$ , only the first term ( $n=0$ ) is left, with  $2R_0=1$ . Since all frequencies  $k_n$  go to  $\infty$ , the amplitude of (29) tends to zero. Therefore, decreasing the thickness of the dielectric lining decreases the transverse wake potential without affecting the amplitude of the longitudinal wake potential, which simply oscillates faster.

#### Comparison with an infinite periodic disk-loaded structure

The case  $L=\infty$ , i.e. a single cell on an infinite beam-pipe, has been treated completely [1]. More recently Glückstern [4] derived the

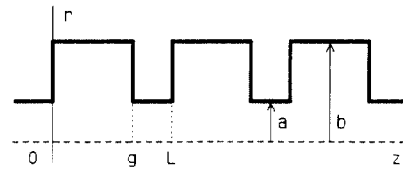


Fig. 3 Geometry of a periodic disk-loaded structure

first terms of an asymptotic expansion of  $Z_{\parallel}(\omega)$  for  $L$  finite and  $m=0$ ; it reads:

$$Z_{\parallel}(\omega) = \frac{\zeta_0}{\pi} \frac{1}{jka^2} \left[ 1 + \left( \frac{jka^2}{2\pi g} \right)^{-\frac{1}{2}} \frac{L}{g} + \dots \right]^{-1} \quad m=0, \quad \frac{b}{a} = \infty \quad (30)$$

The corresponding wake potential per unit length of the structure is still given by (9), with

$$v(s) = H(s) \left[ 1 + 2 \left( \frac{2sg}{\beta a^2} \right)^{\frac{1}{2}} \frac{L}{g} + \dots \right]^{-1} \quad m=0, \quad s < \min(2g, s_3) \quad (31)$$

where [1]

$$s_3 = \beta \sqrt{(2b-2a)^2 + g^2} - g \quad (32)$$

If we compare (31) with (14) for a dielectric-lined structure, we see that  $v(0+)=1$  in both cases, but the longitudinal wake potential drops more rapidly with  $s$  in the disk-loaded structure. To make a disk-loaded structure efficient as a wake-field accelerator, one must have  $L/g \approx 1$  and  $g/a$  as small as possible.

It is not possible to derive the transverse wake potential by integrating (31) with respect to  $s$ , because (31) applies in a neighbourhood of  $s=0$  which is too small; but we can obtain an upper limit for  $w_{\perp}(s)$  when dividing the value for a single cell [1] by  $L$ . The result is an upper bound which is identical to (27) except for an extra factor close to  $\epsilon_m$  [2].

When  $s > s_3$ , the reflections at  $r=b$  begin to influence the test particle, and  $w_{\perp}(s)$  is represented by a series similar to (29), where (19) always applies. In contrast to the dielectric structure

however, although they decrease with  $n$  as  $k_n^{-\frac{3}{2}}$  on the average, the  $R_n$ 's now fluctuate wildly with  $n$ . Depending on  $b/a$  and  $g/a$ , some of the first  $R_n$ 's may take values larger than the ones for the dielectric structure. If the exciting charge is not point like and therefore excites mainly the lower frequencies, it can happen that the wake potential (longitudinal or transverse) appears to be larger in a disk-loaded structure, although for a point charge  $Q$  exciting all frequencies, the wake potentials reach peak values which are comparable in both structures.

#### Acknowledgement

The numerical computations mentioned in the text have all been performed by L. Verolino.

#### References

- [1] G.Dôme: Wake potentials of a relativistic point charge crossing a beam-pipe gap: an analytical approximation, IEEE Transactions on Nuclear Science, Vol. NS-32, October 1985, p.2531-2534.
- [2] G.Dôme: The dielectric-lined structure, CERN Report SL/90-41(RFS), 1990
- [3] K.Y. Ng: Wake fields in a dielectric-lined waveguide, Fermi Lab report FN-533, March 1990.
- [4] R.L. Glückstern: Longitudinal impedance of a periodic structure at high frequency, Physical Review D, Vol. 39 (1989), p. 2780-2783.